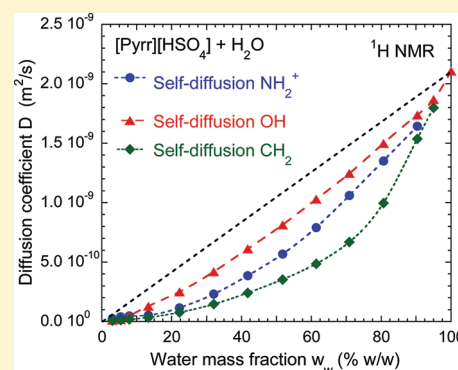


Transport Properties Investigation of Aqueous Protic Ionic Liquid Solutions through Conductivity, Viscosity, and NMR Self-Diffusion Measurements

Mérièm Anouti,^{*,†} Johan Jacquemin,[‡] and Patrice Porion[§][†]Laboratoire PCMB (EA 4244), équipe (CIME), Université François Rabelais, Parc de Grandmont 37200 Tours, France[‡]The QULL Research Centre, School of Chemistry and Chemical Engineering, Queen's University of Belfast, Stranmillis Road, Belfast BT9 5AG, United Kingdom[§]Centre de Recherche sur la Matière Divisée, CNRS-Université d'Orléans, UMR6619, 1b rue de la Férollerie, 45071 Orléans Cedex 2, France

ABSTRACT: We present a study on the transport properties through conductivity (σ), viscosity (η), and self-diffusion coefficient (D) measurements of two pure protic ionic liquids—pyrrolidinium hydrogen sulfate, [Pyr][HSO₄], and pyrrolidinium trifluoroacetate, [Pyr][CF₃COO]—and their mixtures with water over the whole composition range at 298.15 K and atmospheric pressure. Based on these experimental results, transport mobilities of ions have been then investigated in each case through the Stokes–Einstein equation. From this, the proton conduction in these PILs follows a combination of Grotthuss and vehicle-type mechanisms, which depends also on the water composition in solution. In each case, the displacement of the NMR peak attributed to the labile proton on the pyrrolidinium cation with the PILs concentration in aqueous solution indicates that this proton is located between the cation and the anion for a water weight fraction lower than 8%. In other words, for such compositions, it appears that this labile proton is not solvated by water molecules. However, for higher water content, the labile protons are in solution as H₃O⁺. This water weight fraction appears to be the solvation limit of the H⁺ ions by water molecules in these two PILs solutions. However, [Pyr][HSO₄] and [Pyr][CF₃COO] PILs present opposed comportment in aqueous solution. In the case of [Pyr][CF₃COO], η , σ , D , and the attractive potential, E_{pot} , between ions indicate clearly that the diffusion of each ion is similar. In other words, these ions are tightly bound together as ion pairs, reflecting in fact the importance of the hydrophobicity of the trifluoroacetate anion, whereas, in the case of the [Pyr][HSO₄], the strong H-bond between the HSO₄[−] anion and water promotes a drastic change in the viscosity of the aqueous solution, as well as on the conductivity which is up to 187 mS·cm^{−1} for water weight fraction close to 60% at 298 K.



1. INTRODUCTION

Ionic liquids (ILs) are molten salts that can be found in the liquid state at a wide temperature range including, generally the room temperature. Due to their unique physical and chemical properties, like high thermal stability, tunable solubility for a diverse range of solutes, and extremely low vapor pressure, ILs can be used as solvents for catalysis, synthesis, and extraction as an alternative to organic compounds in industrial processes.^{1–8} ILs can be used to reduce or eliminate the hazards of volatile organic solvents.^{9,10} Furthermore, ILs are also extremely studied as electrolytes for electrochemical processes, as well as for enzyme catalysis multiphase bioprocess operations.^{9,11} To date, ionic liquids are generally classified into two broad categories, i.e., aprotic ionic liquids (AILs) and protic ionic liquids (PILs).¹² The PILs subgroup is defined when the selected IL is formed by simple transfer of a proton from a Brønsted acid to a Brønsted base. When a PIL is synthesized by mixing a strong acid with a strong base, the proton is fixed very tightly to the base; in this case, the PIL is most likely composed

entirely of ions with possible ion complexation and aggregate formation.¹³

To design any process involving ILs on an industrial scale, it is necessary to know some thermophysical properties, such as viscosity, conductivity, and diffusivity. Furthermore, these experimental data provide also useful fundamental information about molecular interactions and are also applied to evaluate thermodynamic models.^{14,15} These models provide then a better understanding of the nature of molecular aggregation that exists in the binary mixtures. However, the relatively high viscosities of pure ILs in comparison with traditional solvents has resulted in limited commercial use to date. This problem is partially resolved by mixing ILs with water or organic solvents.^{16–19} In fact, the main advantage of using (PIL + molecular solvent) binary mixtures is to decrease the viscosity and increase the conductivity of the solution, which leads to

Received: November 12, 2011

Published: March 9, 2012

lowering the energy requirements for any engineering process.^{16,18} In other words, the development of knowledge of the physical properties of (PILs + molecular solvent) mixtures is extremely important, especially their transport properties, which are crucial and have importance from practical and/or theoretical points of view. Although applications of PILs are well-known, a detailed knowledge of the thermodynamic behavior of (PILs + molecular solvent) mixtures has not yet received a particularly large share of the literature based on ionic liquids studies,^{20–31} and is still limited.^{32–34} A high ionic concentration, resulting in significant Coulombic interactions, implies that the differences in the ionic state and ion dynamics significantly contribute to the variations in their physicochemical properties. However, to date, available microscopic information into the literature regarding the ionic state and ion dynamics is still insufficient. It was only recently recognized that the pulsed field gradient spin–echo (PGSE) nuclear magnetic resonance (NMR) method could be applied in order to determine the self-diffusion coefficients of individual ionic species in ILs solutions.^{35–37} In this context, it is important to investigate transport phenomena in different ILs solutions over a wide range of temperature, not only from an engineering viewpoint but also to obtain more fundamental knowledge.

We present herein the transport properties, i.e., the conductivity (σ), viscosity (η), and self-diffusion coefficients (D) measurements of two pure PILs—pyrrolidinium hydrogen sulfate, [Pyr][HSO₄], and pyrrolidinium trifluoroacetate, [Pyr][CF₃COO]—and their mixtures with water over the whole composition range at 298.15 K and atmospheric pressure. The outstanding feature of this paper is to provide a complete set of their transport properties data as a function of composition in aqueous solution. Different experimental measurements have been investigated to obtain both properties like the self-diffusion coefficient for cation and anions using pulsed-gradient spin–echo nuclear magnetic resonance (PGSE-NMR) measurements, as well as the ionic conductivity and the shear viscosity using a multifrequencies conductimeter and cone–plate rheometer experiments, respectively. Comparisons of the self-diffusion with either the conductivity or the viscosity are then examined based on the Nernst–Einstein and Stokes–Einstein equations, respectively, from which, information about the degree of cation–anion associations and temperature effects on the self-diffusion coefficients are then reported and commented in detail.

2. EXPERIMENTAL SECTION

2.1. Materials. Pyrrolidine (GC grade, molecular purity >99.0%), sulfuric acid (molecular purity 68% in water) solution, trifluoric acid (GC grade, molecular purity >99.0%), and 1,2-dichloroethane (DCE) (GC grade, molecular purity >99.0%) purchased from Sigma-Aldrich were used without further purification. Prior to use, water was purified with a Milli-Q 18.3 M Ω water system.

2.2. Preparation of PILs and Aqueous Solutions. Pyrrolidinium trifluoroacetate, [Pyr][CF₃COO], and pyrrolidinium hydrogen sulfate, [Pyr][HSO₄], were synthesized by mixing each corresponding acid with the pyrrolidine in equimolar conditions according to the procedure described in a previous publication.³⁸ Since both PILs were very hygroscopic compounds, PILs samples were dried overnight at 343 K under high vacuum (1 Pa) prior to their characterizations. PILs were analyzed for water content using coulometric Karl Fischer

titration prior to the measurements. In the case of the [Pyr][CF₃COO], the water content was close to 6000 ppm (0.6% w_w) just after its distillation using DCE, and this value increased up to 22 000 ppm (2.2% w_w) after a few weeks since this PIL forms an eutectic mixture with water. In the case of the [Pyr][HSO₄], the water content varied from 200 to 30 000 ppm (0.2–3.0% w_w) after storing of this PIL for several weeks. For each PIL, its binary mixtures samples with water were prepared by addition of pure PIL into distilled water with a step Δw_w of 5%.

2.3. Measurements. Viscosities were measured using a TA Instruments rheometer (AR 1000) with cone-plan geometry at 298.15 K. The temperature in the cell was regulated within ± 0.01 K with a solid-state thermostat. The viscosity measurements of the PILs in aqueous solutions were carried out by preparing different (PIL + water) binary mixtures over the whole composition range at 298.15 K. Viscosity standard (Brookfield, 12700 cP at 298.15 K) and water were used to calibrate the rheometer. From this study, the uncertainty of viscosity measurements did not exceed $\pm 1\%$.

Conductivities were performed by using a Crison (GLP 31) digital multifrequencies conductimeter. The temperature control at $T = 298.15$ K was carried out ± 0.02 K by means of a JULABO thermostated bath. The conductimeter was calibrated with standard solutions of known conductivity (0.1 and 0.02 mol·L^{−1}, KCl). The conductivity measurements of the PILs in aqueous solutions were carried out by continuous addition of pure PILs into water. Each conductivity was recorded when its stability was better than $\pm 1\%$ within 2 min, and the uncertainty of reported conductivities did not exceed $\pm 2\%$.

Pulsed-Gradient Spin–Echo NMR (PGSE-NMR). All the PGSE-NMR experiments were performed on a Bruker DSX100 spectrometer with a 2.35 T superconducting magnet (Larmor frequencies $\nu_0 = 100.13$ MHz for ¹H and $\nu_0 = 94.22$ MHz for ¹⁹F) equipped with a 10 mm microimaging probe (MicroS Bruker) without a lock system. In order to determine the activation energy for the diffusion process of each ions species, the runs were carried out in a temperature range from 273 to 373 K with an accuracy of ± 1 K and a step $\Delta T = 5$ K. The samples were thermally equilibrated at each temperature for 30 min before any measurements were performed. In addition, and due to the time-consuming nature of such an experimental method, for the binary mixtures, the activation energy was only evaluated for a few aqueous mixtures of [Pyr][HSO₄] (i.e., $w_w = 3.00\%$, 32.07%, and 70.89%). In the case of the [Pyr]-[CF₃COO] sample, the activation energy was only determined for the residual water weight fraction $w_w = 2.2\%$. In this study, to achieve better experimental measurements for these diffusion experiments, the inner diameter of the NMR tube was 6 mm and the liquid height was 10 mm. Indeed, such experimental conditions allow obtaining a good homogeneity of the static magnetic field across the whole PIL solutions. With such conditions, the uncertainty of the reported self-diffusion coefficients did not exceed $\pm 3\%$. Finally, all the chemical shift references were set to a particular arbitrary value for convenience (for more details see the figure captions of the NMR spectra).

The PGSE-NMR method was already used by different research groups to measure the self-diffusion of a variety of ionic species.^{39,40} Herein, for each studied PIL, cationic and anionic self-diffusion coefficients were determined by proton (¹H) and/or fluorine (¹⁹F) NMR, respectively. Because of the

difference between the longitudinal relaxation time (T_1) and the transverse relaxation time (T_2) (T_2 values are usually shorter than T_1), a modified stimulated spin-echo sequence was used.⁴¹ It consisted of a 13-interval PGSTE pulse sequence⁴² with a bipolar-gradient pair to improve the self-diffusion coefficient measurements (Figure 1). Indeed, at high temperatures ($T > 358$ K) in such media, the T_1/T_2 ratio in ^1H NMR can exceed 25 for certain chemical groups of the PILs. For example, at high temperature ($T = 373$ K) for the methyl group of the pyrrolidinium cation in $[\text{Pyr}][\text{CF}_3\text{COO}]$, the relaxation times T_1 and T_2 (^1H NMR) are 1160 and 41 ms, respectively, and the ratio T_1/T_2 reaches 28.3.

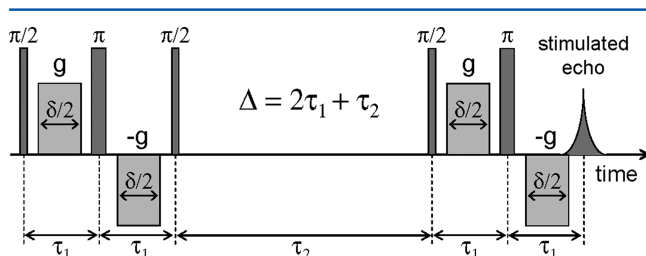


Figure 1. A schematic view of the 13-interval PGSTE-NMR pulse sequence. This NMR sequence produced a stimulated spin-echo at the time $t = 4\tau_1 + \tau_2$. The diffusion time is defined by $\Delta = 2\tau_1 + \tau_2$.

By using the PGSE-NMR method, self-diffusion coefficients were calculated by measuring the decrease of the NMR echo signal intensity through increasing magnetic field gradients (g). Self-diffusion coefficients, D , were then obtained by a simple linear least-squares fitting of the echo attenuation $E(g, \Delta)$ according to eq 1

$$E(g, \Delta) = I(g, \Delta)/I(0, \Delta) \\ = \exp[-\gamma^2 g^2 \delta^2 D (\Delta - \delta/3)] \quad (1)$$

where $I(g, \Delta)$ and $I(0, \Delta)$ are the echo intensities measured with and without the field gradient g (varying between 0 and g_{\max}), respectively. δ is its duration, γ is the gyromagnetic ratio of the nuclei, Δ is the diffusion time (fixed to 20 ms), and D is the self-diffusion coefficient.

For all ^1H and ^{19}F PGSTE-NMR runs, the magnetic field gradient duration (δ) was set to 3 ms and the maximum value of the magnetic field gradient (g_{\max}) was 1.5 T/m. Depending on the longitudinal relaxation time T_1 value, the recovery delay was varied between 2 and 10 s. In addition, the spectrometer dead time was 100 and 350 μs , in ^1H and ^{19}F NMR measurements, respectively.

3. RESULTS AND DISCUSSION

3.1. Conductivities of (PIL + Water) Binary Systems.

The ionic conductivity values for (PIL + water) binary systems were measured at 298.15 K, as function of the water weight fraction percentage, w_w . The data for specific conductivity, σ , for the studied solutions are presented in Table 1 and are illustrated in Figure 2.

Figure 2 shows in each case that irrespective of the nature of the selected anion, the ionic conductivity presents a maximum value as the function of the water weight fraction, from which the anion effect on the conductivity of studied aqueous solutions can be analyzed. Maxima of conductivity, σ_{\max} , are obtained for $\sigma_{\max} = 44.20 \text{ mS}\cdot\text{cm}^{-1}$ at $w_{w(\max)} = 0.5$ and for $\sigma_{\max} = 187.30 \text{ mS}\cdot\text{cm}^{-1}$ at $w_{w(\max)} = 0.65$, in the case of binary mixtures containing $[\text{Pyr}][\text{CF}_3\text{COO}]$ and $[\text{Pyr}][\text{HSO}_4]$, respectively. In other words, each maximum of conductivity is not obtained for the same water composition, $w_{w(\max)}$, which depends essentially on the nature of the selected anions. In the whole composition range, $[\text{Pyr}][\text{HSO}_4]$ aqueous solutions present higher conductivities than the $[\text{Pyr}][\text{CF}_3\text{COO}]$ ones. Additionally, in each case, the presence of water increases the ionic conductivity of the solution in comparison with the value reported for the pure PIL. In comparison with the conductivity

Table 1. Specific (σ) and Molar (Λ) Ionic Conductivities for the Binary Mixtures of (PIL + Water) as a Function of Water Weight Fraction Percentage, w_w , and of the Solution Concentration Square Root, \sqrt{C} ($\text{mol}\cdot\text{L}^{-1}$)^{1/2} at 298.15 K

[Pyr][HSO ₄]				[Pyr][CF ₃ COO]			
w_w (%)	σ (mS·cm ⁻¹)	\sqrt{C} (mol·L ⁻¹) ^{1/2}	Λ (S·cm ² ·mol ⁻¹)	w_w (%)	σ (mS·cm ⁻¹)	\sqrt{C} (mol·L ⁻¹) ^{1/2}	Λ (S·cm ² ·mol ⁻¹)
3	5.53	7.29	0.55	2	8.23	2.33	1.52
5	15.07	6.03	1.24	6	17.28	2.25	3.39
10	29.30	5.19	2.35	15	26.40	2.00	8.67
16	53.80	4.58	3.93	20	30.50	1.90	10.99
20	72.90	4.10	5.46	25	34.30	1.81	13.01
26	91.80	3.54	9.89	30	37.90	1.71	15.09
30	112.80	2.53	26.81	35	40.50	1.51	19.34
32	124.2	2.02	45.73	40	42.45	1.30	23.83
33	130.7	1.50	78.87	45	43.75	1.25	25.25
47	171.9	1.03	125.67	50	44.20	1.20	26.44
51	178.10	0.73	170.49	55	44.20	1.14	28.55
59	186.60	0.70	176.68	60	43.80	1.09	29.41
65	186.50	0.67	182.24	66	41.90	1.05	30.42
70	180.90	0.64	188.21	71	39.80	1.00	31.75
76	168.60	0.61	193.82	76	37.50	0.96	32.86
81	151.70	0.57	204.30	79	33.80	0.90	34.49
86	125.60	0.53	213.16	85	28.20	0.83	36.63
91	97.00	0.50	220.96	90	20.60	0.72	39.45
95	65.50	0.47	227.69	94	13.58	0.55	44.81
100	0.00	0.42	245.02	100	0.06	0.46	49.79

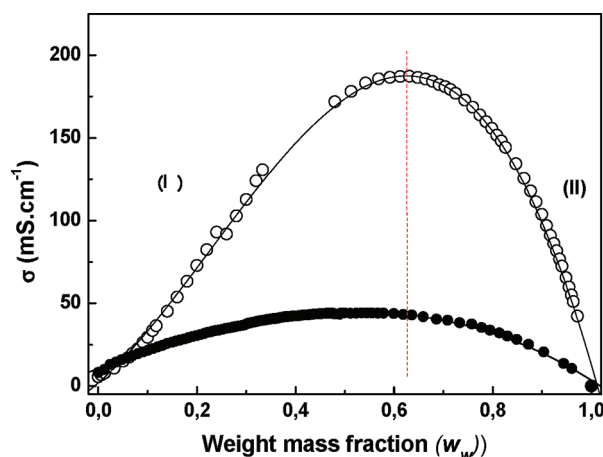


Figure 2. Ionic conductivity, σ , of aqueous PILs solutions as the function of the water weight fraction, w_w . \circ , [Pyr][HSO₄]; \bullet , [Pyr][CF₃COO].

of pure PILs, the conductivities of solutions at the $w_{w(\max)}$ composition increase up to 5.4 and 33.8 times for binary systems containing the [Pyr][CF₃COO] and the [Pyr][HSO₄], respectively.

However, the similarity between the two curves of the conductivity as a function of composition reported in Figure 2 indicates that the charge transport mechanisms must be the same for both (PIL + water) mixtures. When water is added to a pure PIL, its charge density is then reduced as well as its viscosity. In each case, after the $w_{w(\max)}$ composition, the dilution effect of water becomes more predominant. In fact, according to this conductivity profile, Figure 2 can be subdivided in two markedly different regions depending to the water concentration, which can be lower or higher than the $w_{w(\max)}$ composition. Although, the effect of Coulombic interionic interactions is a monotonic reduction of the mobility of ionic charges in bulk electrolyte solutions over the whole range of concentration. In the first region (denoted I in Figure 2, i.e., $w_w < w_{w(\max)}$), the ionic charges can be considered as high-mobility charge carriers; in fact, the addition of water to the bulk solution results in an increase of the conductivity of the solution. In the second region (denoted II in Figure 2, i.e., $w_w > w_{w(\max)}$), due to the dilution effect, the mobility of the charge carriers is considerably lower, which causes a decrease of the ions interactions, and in fact a decrease of the conductivity of the solution. This region II can be also analyzed by using conventional transport theory in ionic solutions, thereby treating the medium as a statistical (or diffuse) distribution of ionic charges in a uniform structure less continuum, while in region I, the similarity to the pure IL is progressively less marked. According to Molenat, the existence of a maximum of conductivity/concentration profile must be understood in the electrolyte-like context of the region I.⁴³

To our best knowledge, a satisfactory quantitative theoretical explanation of the maximum of the curve $\sigma = f(w_w)$ and its position for each salt does not exist, even in the electrolyte solution transport theory, even if some works explain this maximum by the presence of a glassy transition in the aqueous solution at different concentrations around this maximum.⁴⁴ Vila et al. have shown that in the electrical conduction two different mechanisms are present.⁴⁵ One of them is the number of ions present in the transport charges (which increases with the PIL concentration). The other one is related to the mobility

of the ions in the solution, which will be lower when the number of ions increases (which decreases with the concentration). In the maximum of the curve, the addition of both effects is optimal; consequently the conduction is most effective.^{46,47}

The molar conductivities, Λ (S·cm²·mol⁻¹), of the PILs in aqueous solutions were then calculated from the ionic conductivity σ (mS·cm⁻¹) and the molar concentration. The dependence of the molar conductivity (Λ) on the square root of the PIL mole concentration ($C_{IL}^{1/2}$) is illustrated for studied PILs aqueous solutions in Figure 3.

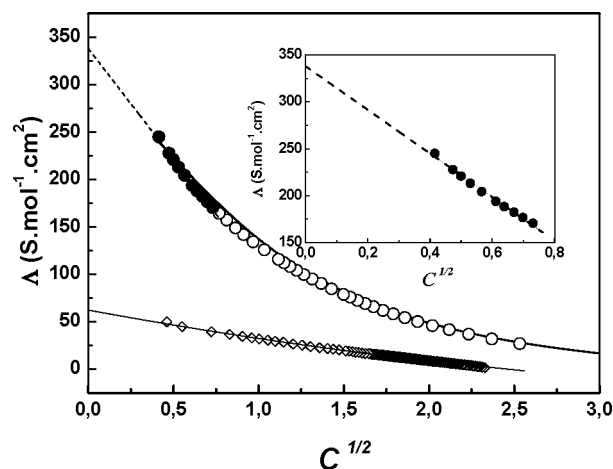


Figure 3. Debye–Onsager plot of molar conductivity, Λ , against $C_{IL}^{1/2}$ for pyrrolidinium-based PILs in aqueous solutions: \circ , [Pyr][HSO₄]; \diamond , [Pyr][CF₃COO]. The inset figure represents the molar conductivity, Λ , vs $C_{IL}^{1/2}$ at low concentrations in the case of the [Pyr][HSO₄].

From Figure 3, we observed that the behavior of the curve is different according to the nature of the PIL. For pyrrolidinium hydrogen sulfate at high PIL concentrations, i.e., $C_{IL} > 1.0$ mol·L⁻¹, Λ decreases exponentially when $C_{IL}^{1/2}$ increases. This behavior is characteristic of a weak electrolyte, i.e., partially associated in water, whereas the trifluoroacetate-based PIL presents a behavior corresponding to a strong electrolyte, i.e., totally dissociated in water. To determine the infinite dilution conductivity of PILs cation and anions, we plot the molar conductivity, Λ , versus $C_{IL}^{1/2}$ at low concentrations, as shown in the case of the [Pyr][HSO₄] in the insert plot of the Figure 3. The obtained graphs represent a high linearity which is the expected behavior at infinite dilution⁴⁸ according to the Debye–Onsager relation

$$\Lambda = \Lambda^0 + (a\Lambda^0 + b)\sqrt{C_{IL}} \quad (2)$$

where Λ is the molar conductivity, Λ^0 is the infinite dilution molar conductivity, C_{IL} is the PIL molar concentration, and a and b are two empirical constants.

The infinite dilution molar conductivities of the different PILs, Λ^0 , were first determined by fitting the experimental data presented in Table 1 using eq 2. In order to evaluate the infinite dilution conductivity of the investigated cation or anions, the additivity law at infinite dilution was applied through the following relationship:

$$\Lambda^0 = z_+\Lambda_+^0 + z_-\Lambda_-^0 \quad (3)$$

The hydrogen sulfate HSO_4^- anion has the largest value of the infinite dilution molar conductivity, which is close to $\Lambda_-^0 = 300 \text{ S}\cdot\text{cm}^2\cdot\text{mol}^{-1}$. The smallest values of the infinite dilution molar conductivity have been found in the case of the pyrrolidinium cation with $\Lambda_+^0 = 60 \text{ S}\cdot\text{cm}^2\cdot\text{mol}^{-1}$, as well as in the case of and the trifluoroacetate CF_3COO^- anion with $\Lambda_-^0 = 5.1 \text{ S}\cdot\text{cm}^2\cdot\text{mol}^{-1}$. The reported infinite dilution molar conductivity values are in excellent agreement with values reported by others in the case of these studied anions,⁴⁹ and by our group in the case of the pyrrolidinium cation in a previously work.⁵⁰

Self-diffusion of PILs in water can be also considered as the diffusion of a binary univalent electrolyte. Consequently, by applying the Nernst–Haskell equation,⁴⁸ the diffusion coefficient of electrolytes is calculated as

$$D_{\text{PIL}}^0 = \frac{RT}{F^2} \frac{|z_+| + |z_-|}{|z_+z_-|} \frac{\Lambda_+^0 \Lambda_-^0}{\Lambda_+^0 + \Lambda_-^0} \quad (4)$$

where D_{PIL}^0 is the diffusion coefficient of PILs in water at infinite dilution, R the gas constant, T the absolute temperature, and F Faraday's constant, and z_+ and z_- are the charge numbers of cation and anion, respectively. Λ_+^0 and Λ_-^0 are the infinite dilution conductivities of the cation and anion, respectively. From this, $D_{\text{PIL}}^0 = 2.663 \times 10^{-9} \text{ m}^2\cdot\text{s}^{-1}$ and $D_{\text{PIL}}^0 = 2.504 \times 10^{-10} \text{ m}^2\cdot\text{s}^{-1}$ were obtained at infinite dilution in the case of aqueous solutions of $[\text{Pyr}][\text{HSO}_4]$ and $[\text{Pyr}][\text{CF}_3\text{COO}]$, respectively. These values could be compared to those obtained by pulsed-gradient spin–echo NMR (PGSE-NMR) as reported in the next subsection (see section 3.3.1).

3.2. Viscosities of (PIL + Water) Binary Systems. Since ILs are more viscous than conventional solvents, in most applications they can be used in mixtures with other less viscous fluids. Therefore, the viscosity of pure ILs and their mixtures with conventional solvents is an important property and their knowledge is primordial for any industrial processes. Viscosities of (PIL + water) binary mixtures were measured at 298.15 K. Experimental data of dynamical viscosity, η , are presented as a function of the PILs mole fraction in Figures 4 and 5.

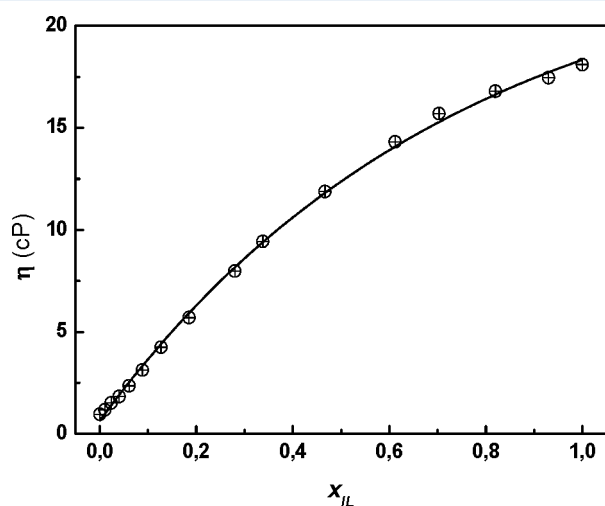


Figure 4. Dynamical viscosity of $([\text{Pyr}][\text{CF}_3\text{COO}] + \text{H}_2\text{O})$ binary system as a function of PIL mole fraction. The solid line represents the Seddon-type fitting⁵¹ with the parameters indicated in eq 6a.

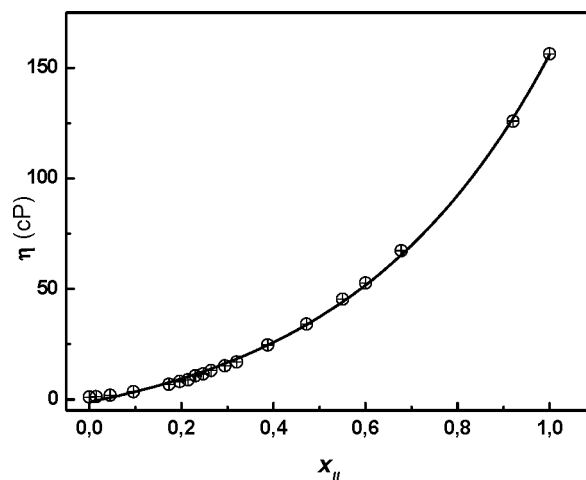


Figure 5. Dynamical viscosity of $([\text{Pyr}][\text{HSO}_4] + \text{H}_2\text{O})$ binary system as a function of PIL mole fraction. The solid line represents the Seddon-type fitting⁵¹ with the parameters indicated in the eq 6b.

To correlate the variation of the viscosity with the composition, Seddon et al.⁵¹ have stated that viscosities for ionic liquid mixtures with molecular solvents can generally be described by the following exponential expression

$$\eta = \eta_0 \exp\left[\frac{-x_w}{a}\right] \quad (5)$$

where η_0 is the dynamical viscosity of the pure IL, x_w is the mole fraction of the solvent (water in our case), and a is a fitting parameter which depends on the types of IL and solvent. Each solid line shown in Figures 4 and 5 represents the fitted curve using eq 5 with parameters reported in eqs 6a and 6b for binary mixtures containing the $[\text{Pyr}][\text{HSO}_4]$ and the $[\text{Pyr}][\text{CF}_3\text{COO}]$, respectively.

$$\eta = \eta_0 \exp\left(-\frac{x}{a}\right), \quad \eta_0 = 0.023, \quad a = 0.7404, \quad R^2 = 0.997 \quad (6a)$$

$$\eta = \eta_0 \exp\left(-\frac{x}{a}\right), \quad \eta_0 = 0.0013, \quad a = -0.44, \quad R^2 = 0.999 \quad (6b)$$

From Figures 4 and 5, it appears that the addition of water in PIL solutions decreases the viscosity of the media in comparison with the viscosity of pure PILs. For example, the viscosity of pure $[\text{Pyr}][\text{HSO}_4]$ is close to 156.3 cP, whereas its mixture with water at the equimolar composition has a viscosity close to 33 cP. Additionally, for high concentration of PIL ($x_{\text{IL}} > 0.5$) the choice of the anion affects also dramatically the viscosity of the solution. This effect is driven by the fact that the HSO_4^- -based PIL is around 9 times more viscous than the PIL containing the CF_3COO^- anion. For lower PIL mole fraction, such difference tends to decrease, since the viscosity of each aqueous solution tends to converge until the viscosity of pure water.

The viscosity deviations from ideal η^E were calculated from eq 7

$$\eta^E = \eta - (x_1\eta_1 + x_2\eta_2) \quad (7)$$

where x_1 and x_2 are the mole fractions of $[\text{Pyr}][\text{X}]$ (with $\text{X} = \text{HSO}_4^-$ and CF_3COO^-) and of the water. η , η_1 , and η_2 are the viscosities of the mixture, the pure IL, and water, respectively.

Figure 6 shows the dependence of the viscosity deviations as a function of the PIL mole fraction composition, x_{PIL} , at 298.15 K. It can be seen that, in the case of the $([\text{Pyr}][\text{CF}_3\text{COO}] + \text{H}_2\text{O})$ binary mixture, η^{E} is positive over the entire composition range with small amplitude (maximum $\eta^{\text{E}} = 3$ cP), whereas, for the $([\text{Pyr}][\text{HSO}_4] + \text{H}_2\text{O})$ binary mixture, η^{E} is negative in the whole composition range with high amplitude (maximum η^{E} close to -40 cP), which is 14 times higher than the maximum viscosity deviation value reported in the previous case. In fact, the strong ionic association and the hydrophobicity of the fluorinated anion could explain the low impact of the addition of water on the viscosity of the trifluoroacetate-based PIL solution. In contrast, the acidic equilibrium of HSO_4^- anion and water promotes a drastic change in viscosity. These results are consistent with changes in conductivity observed in Figure 2.

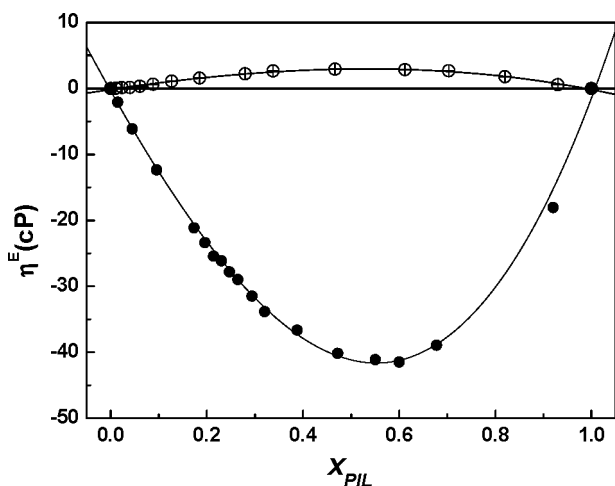


Figure 6. Comparison of the viscosity deviations from ideality, η^{E} , as a function of the PIL mole fraction for binary systems: ●, $([\text{Pyr}][\text{HSO}_4] + \text{H}_2\text{O})$; ○, $([\text{Pyr}][\text{CF}_3\text{COO}] + \text{H}_2\text{O})$ at 298.15 K.

3.3. Pulsed-Gradient Spin–Echo NMR (PGSE-NMR).

Self-Diffusion Coefficient Measurements. *Characterization of Neat PILs and (PIL + Water) Binary Systems by 1D NMR Spectroscopy.* Water is one of the most commonly occurring impurities in ILs, which may dramatically influence the physicochemical properties of PILs. Water molecules and its quantities change the IL structure by introducing water–cation interactions in addition to the cation–anion interactions already present. ^1H NMR combined with fluorescence spectroscopy was successfully utilized to investigate (IL + water) systems of several ionic liquids.⁵² In this work, to determine the nature of the water–cation interactions, as well as the sites of water binding to the PILs, the ^1H NMR spectra, performed at 100 MHz, were investigated with the assignments of the different chemical groups in both compounds as presented in Figure 7.

The largest difference between the two spectra is the sharpness of the peak attributed to the labile hydrogen on the nitrogen atom. In the case of $[\text{Pyr}][\text{HSO}_4]$, the peak is thinner which is synonymous with a more pronounced localization of the proton between the anion and cation. This may very well be understood because of the strong interactions of the proton with the hydrogen sulfate anion. Additionally, the peak assigned to water molecules (OH) is shifted to the high value of chemical shift, which means that water molecules are near to the HSO_4^- anion.

Figure 8 shows the water weight fraction w_w dependencies of the different ions using the ^1H and ^{19}F nuclei self-diffusion coefficients measurements in $([\text{Pyr}][\text{HSO}_4] + [\text{H}_2\text{O}])$ binary mixture. At low w_w values (between 3% and 13.33% w/w), in the case of the NH_2^+ and OH chemical groups, one can observe a variation of the position for their resonance line. At $w_w = 7.8\%$ only one peak is observed at $\delta_{\text{H}} = 6$ ppm, which is attributed to solvated labile proton by water (H_3O^+). Before this weight fraction, the labile protons are localized between the nitrogen atom of pyrrolidinium cation and the oxygen atom of the hydrogen sulfate anion. $w_w = 8\%$ appears to be the limit of the H^+ ions solvation by water molecules. At a very low water content, the interaction of water with the PIL was highly specific and was localized, in contrast, an increasing of the amount of water led to a nonselective solvation.

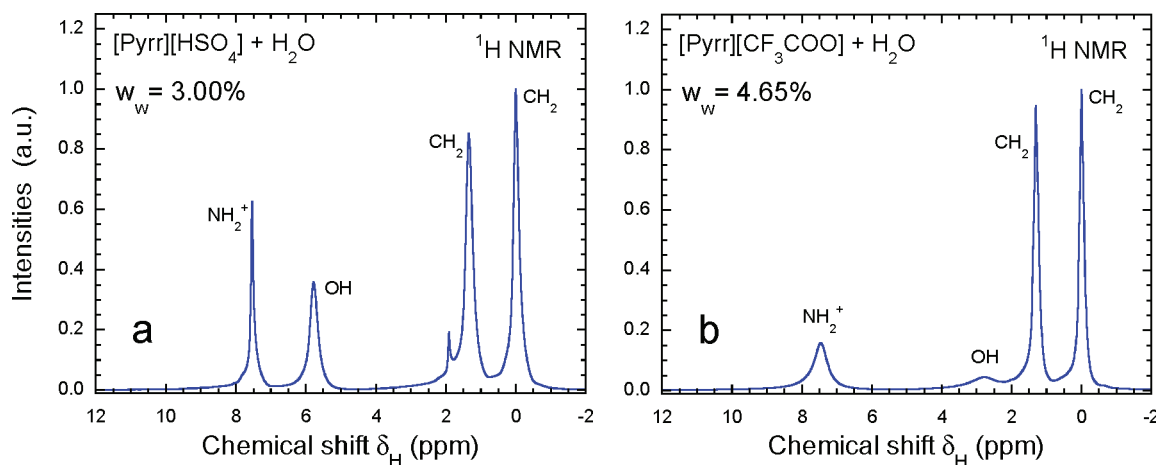


Figure 7. ^1H NMR spectra of (a) $[\text{Pyr}][\text{HSO}_4]$ and (b) $[\text{Pyr}][\text{CF}_3\text{COO}]$ at low water weight fraction for the assignment of the different chemical groups at room temperature ($T = 290$ K). For all the spectra, the chemical shift reference is taken arbitrarily at 0 for the second CH_2 group of the $[\text{Pyr}]$ cation.

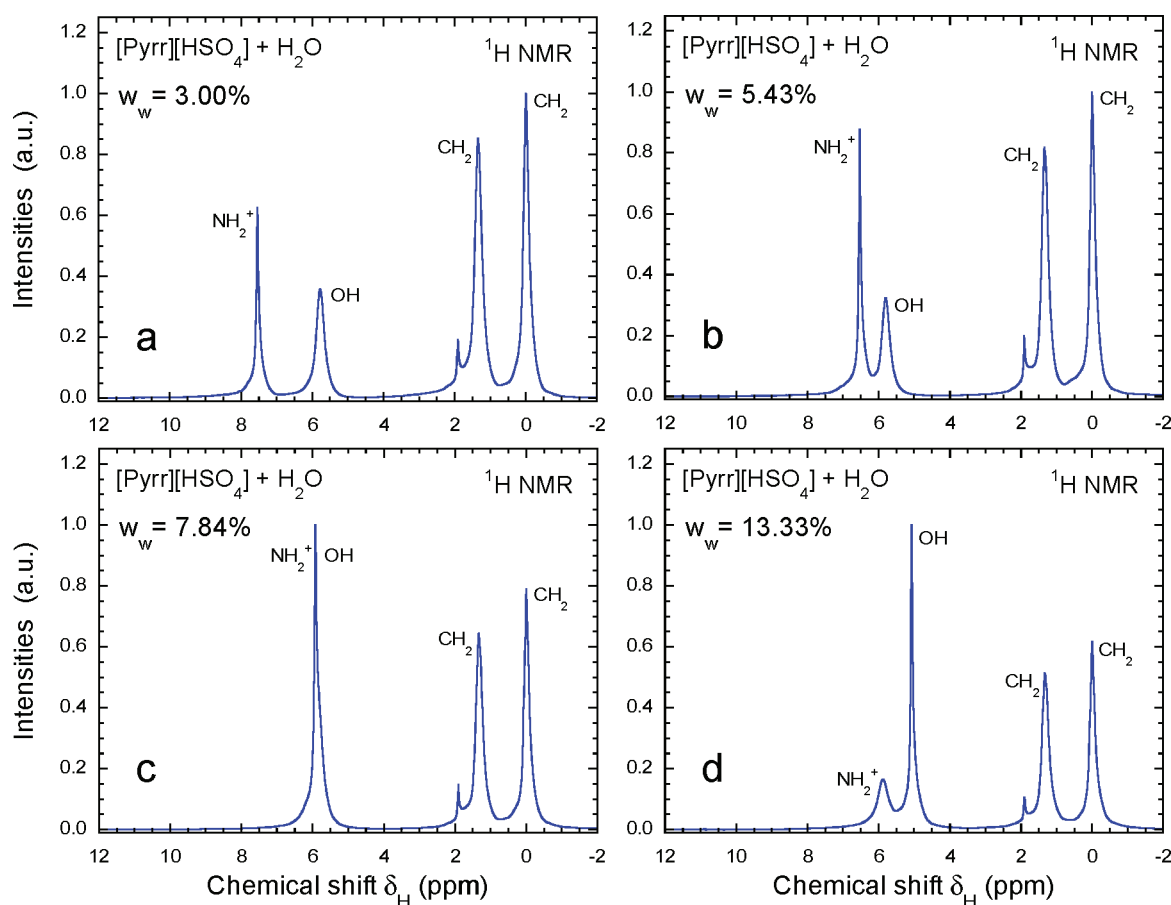


Figure 8. Variations of the ^1H NMR spectra of the binary system $([\text{Pyr}][\text{HSO}_4] + \text{H}_2\text{O})$ as a function of the water weight fraction w_w . For all the spectra, the chemical shift reference is taken arbitrarily at 0 for the second CH_2 groups of the $[\text{Pyr}]$ cation.

Self-Diffusion Coefficient of (PIL + Water) Binary System by ^1H and ^{19}F PGSE-NMR Measurements. Self-diffusion measurements were used as a sensitive test for determining the purity of various ILs.⁵³ It was reported that small amounts of impurity significantly affect transport phenomena in the IL. For example, Rollet et al. report an anomalous diffusion of water in the case of the binary mixture $[\text{bmim}][\text{TFSI}] + \text{water}$ (from 0.3 to 30 mol %), using ^1H and ^{19}F PGSE-NMR. Indeed, the self-diffusion coefficients of all species were found to increase with water content, but compared to the IL ions' behavior, the self-diffusion coefficient of the water molecules increased 25 times greater.⁵³ In other study, Umecky et al.⁵⁴ show that 3% of impurities in commercially available $[\text{bmim}][\text{PF}_6]$ led to a $\approx 25\%$ change in the self-diffusion coefficients of the anion and cation. The PGSE-NMR method allows the determination of the ions' self-diffusion coefficient without the use of any additional probe molecules affecting the diffusion processes. Since the PILs used in this study included NMR-sensitive ^1H and ^{19}F nuclei in the cation and/or anions, each of the cationic and anionic self-diffusion coefficients could be independently determined. Samples studied herein contained initially 30 000 and 22 000 ppm of water in the case of the $[\text{Pyr}][\text{HSO}_4]$ and $[\text{Pyr}][\text{CF}_3\text{COO}]$, respectively. Self-diffusion coefficients D for the different chemical groups (NH_2^+ , OH , CH_2 , and CF_3) as a function of the water weight fraction w_w of the $([\text{Pyr}][\text{HSO}_4] + \text{H}_2\text{O})$ binary system obtained by using ^1H PGSE-NMR measurements at 290 K for selected binary systems are then calculated in all range of concentration. Their deviations to the ideal Raoult's law are

presented in Figures 9 and 10 for $[\text{Pyr}][\text{HSO}_4]$ and $[\text{Pyr}][\text{CF}_3\text{COO}]$ aqueous solutions, respectively.

From Figure 10, it appears that maximum of deviation from ideality is observed for self-diffusion of the cation. This result suggests that pyrrolidinium cation is more affected by water

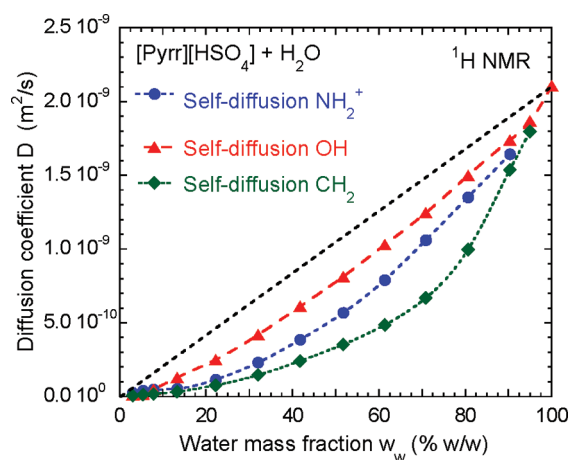


Figure 9. Variations of self-diffusion coefficients D for the different chemical groups (NH_2^+ , OH , and CH_2) as a function of the water weight fraction w_w of the binary system $([\text{Pyr}][\text{HSO}_4] + \text{H}_2\text{O})$ by ^1H PGSE-NMR measurements at 290 K. The black dashed straight line corresponds to the ideal Raoult's law. The other dashed lines are guides for the eyes.

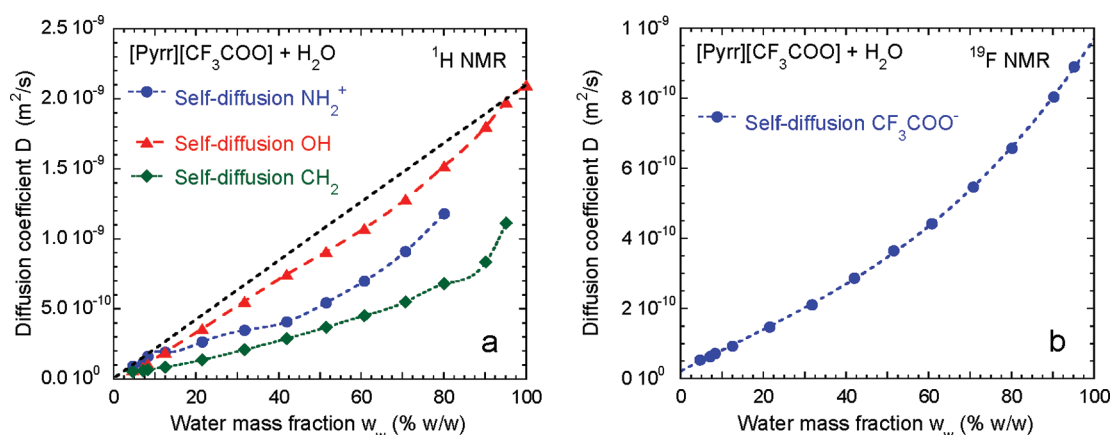


Figure 10. Variations of self-diffusion coefficients D as a function of the water weight fraction w_w in ([Pyr][CF₃COO] + H₂O) binary system at 290 K: (a) NH₂⁺, OH, and CH₂ groups by ¹H PGSE-NMR measurements, (b) CF₃COO[−] group by ¹⁹F PGSE-NMR measurements. The black dashed straight line corresponds to the ideal Raoult's law; the other dashed lines are guides for the eyes.

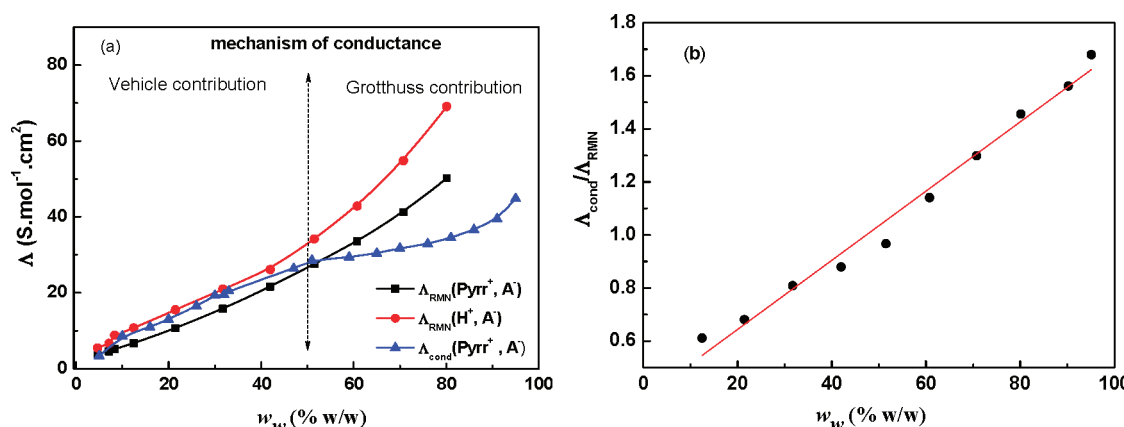


Figure 11. Comparison of molar conductivities Λ_{cond} and Λ_{NMNR} calculated from eqs 3 and 9 for the [Pyr][CF₃COO] + water system. (a) The composition dependency of the molar conductivity Λ_{cond} and Λ_{NMNR} . (b) Molar conductivity ratios ($\Lambda_{\text{cond}}/\Lambda_{\text{NMNR}}$) for [Pyr][CF₃COO] plotted against water weight fraction, w_w .

addition. The comparison of self-diffusion coefficients at infinite dilution determined by PGSE-NMR, $D_{\text{NMNR}} = D_{\text{cation}} + D_{\text{anion}}$, and those calculated by applying the Nernst–Haskell equation show that, in the case of the pyrrolidinium hydrogen sulfate solution, calculated values are in the same order of magnitude ($D_{\text{NMNR}} = 3.2 \times 10^{-9} \text{ m}^2 \cdot \text{s}^{-1}$ and $D_{\text{cond}} = 2.5 \times 10^{-9} \text{ m}^2 \cdot \text{s}^{-1}$), whereas in the case of the pyrrolidinium trifluoroacetate solution, $D_{\text{NMNR}} = 2.0 \times 10^{-9} \text{ m}^2 \cdot \text{s}^{-1}$; such value is 9 times higher than the value calculated by using the Nernst–Haskell equation (i.e., $D_{\text{cond}} = 2.5 \times 10^{-10} \text{ m}^2 \cdot \text{s}^{-1}$). This difference reflects the ionic association of the [Pyr][CF₃COO], since noncharged species do not contribute to the calculation of the D_{cond} .

Several authors have then used self-diffusion coefficients determined by PGSE-NMR to calculate the molar conductivity (Λ_{NMNR}) according to the Nernst–Einstein equation^{55,56}

$$\Lambda_{\text{NMNR}} = \frac{F^2(D_{\text{cation}} + D_{\text{anion}})}{RT} \quad (8)$$

where F is the Faraday constant and R is the universal gas constant.

The self-diffusion coefficients obtained by PGSE-NMR result only from the translational motion (self-diffusion) of the NMR-sensitive nuclei observed. Thus, the Λ_{NMNR} values were derived

from the assumption that all diffusing species detected during the PGSE-NMR measurements contribute to the molar conductivity. On the other hand, the Λ_{cond} values (i.e., the direct current, denoted dc, conductivity) were based on the migration of the charged species under an electric field. Hence, the Nernst–Einstein equation holds only if species involved in diffusion were also responsible for their conduction. In the presence of neutral ion pairs, the Λ_{NMNR} values were expected to differ from those determined by conductivity (Λ_{cond}). Moreover, another important point was that the strong ion–ion interactions occurring in pure or very concentrated PILs solutions should affect the D and Λ values by separate mechanisms and hence to varying extents.

In order to calculate the molar conductivity, it was necessary to take into account all mobile species: the mobile proton (H⁺), the pyrrolidinium ring (Pyr⁺), and the anion (HSO₄[−] or CF₃COO[−]). As the respective contributions of H⁺ and Pyr⁺ to the conductivity were unknown, a parameter α , ranging from 0 to 1, was introduced in the following eq 9:

$$\Lambda_{\text{NMNR}} = \frac{F^2}{RT} ((1 - \alpha)D_{\text{Pyr}^+} + \alpha(D_{\text{H}^+}) + D_{\text{A}^-}) \quad (9)$$

Figure 11a shows the effect of the composition on the calculated molar conductivity, Λ_{NMNR} , using eq 9 in the case of

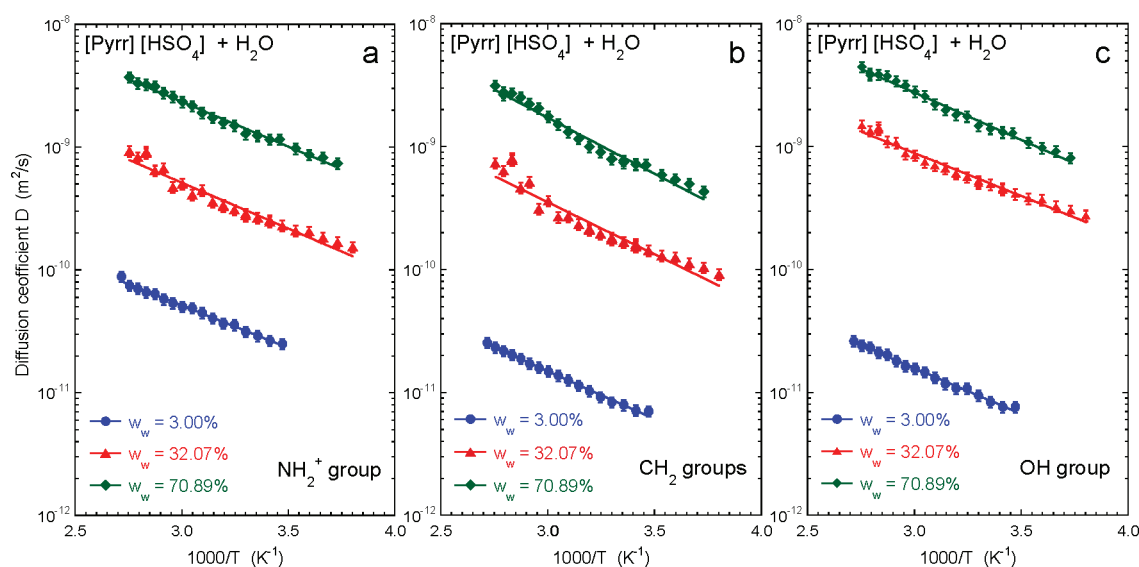


Figure 12. Temperature dependences of ^1H PGSE-NMR self-diffusion coefficients in the binary system $[\text{Pyrr}][\text{HSO}_4] + \text{H}_2\text{O}$ for three selected water weight fractions w_w (3.00, 32.07, and 70.89% w/w): (a) for the NH_2^+ chemical group, (b) for the CH_2 chemical groups, and (c) for the OH chemical group. The solid lines represent the best fit using the Arrhenius law.

the $[\text{Pyrr}][\text{CF}_3\text{COO}]$ aqueous solution, with $\alpha = 1$ and $\alpha = 0$ used as limits. For the sake of comparison, the experimental conductivities Λ_{cond} for $([\text{Pyrr}][\text{CF}_3\text{COO}] + \text{H}_2\text{O})$ binary system have been also plotted in the same graph, as illustrated in Figure 11a. At low composition range (i.e., $w_w < 50\%$ w/w), irrespective of the choice of the α value (e.g., $\alpha = 1$ or $\alpha = 0$), Λ_{cond} was found to be similar to the calculated Λ_{NMR} values. In fact, in this case, ions provide the major contribution to the diffusion in the solution. However, for higher composition range (i.e., $w_w > 50\%$ w/w) it is not the case, since certain discrepancies have been found between calculated and experimental diffusion values. In other words, for such concentrations, the diffusion in solution is certainly driven by the ion pairs, as well as by neutral species, driving in fact that for high composition range (i.e., $w_w > 50\%$ w/w), the Nernst equation becomes invalid. Indeed, the underlying reason for this might be the formation of ion pairs. By assuming that the single ion association and pair dissociation rates are sufficiently fast with the respect to the time scale of the PGSE NMR measurements (10^{-2} – 10^{-3} s), the cation self-diffusivity was then decomposed into two contributions, which correspond to the cation self-diffusivity contributions of the single ion (D_{Pyrr^+}) and of the ion pair (D_{PyrrA}), respectively. Apparently, at low composition range (i.e., $w_w < 50\%$ w/w), both curves corresponding to $\alpha = 1$ and $\alpha = 0$ are almost similar, because the contributions of the Grotthuss is low.

Figure 11b displays the ratio $\Lambda_{\text{cond}}/\Lambda_{\text{NMR}}$ as a function of the water weight fraction, and which was found to be sensitive to changes thereof. Consequently, the $\Lambda_{\text{cond}}/\Lambda_{\text{NMR}}$ ratio indicates the percentage of ions (charged species) contributing to the ionic conduction in the diffusing species. It should be noted here that it was not possible to distinguish the difference between free ions and associated ionic species using the NMR chemical shifts within the NMR time scale (10^{-9} – 10^{-10} s). This implies that the association/dissociation rate of the ionic species, if any, was much faster than the time scale of the dc conductivity measurements used during this work. In the time scale of the conductivity measurements, individual ions under an electrical field migrate for a certain period when ions exist as

charged species, but such ions may associate to form noncharged ion pairs and then aggregate during another period. When the ions form an ion pair, which can be studied as noncharged species, these ions do not contribute in fact to the dc conduction. Thus, $\Lambda_{\text{cond}}/\Lambda_{\text{NMR}}$ ratios can be studied as a measure of the ionic association on the PIL solutions. In the case of $[\text{Pyrr}][\text{CF}_3\text{COO}]$, this association is explained by the strong hydrogen bond between fluorine and hydrogen atoms, and also between hydrogen and nitrogen atoms.

Influence of Temperature on the Self-Diffusion Coefficients. Driver and Johnson⁵⁷ report the dynamic nature of the anionic part on the $[\text{HMIM}][\text{HBr}_2]$ due to the acidic equilibrium of anion in contrast to the cation, where no chemical exchange with the cation was reported using variable-temperature ^1H NMR measurements. In the light of this work, the influence of the temperature on the self-diffusion coefficients has been then quantified by using the Arrhenius equation in the case of the $([\text{Pyrr}][\text{HSO}_4] + \text{H}_2\text{O})$ binary system, particularly for the NH_2^+ , CH_2 , and OH chemical groups at three selected water weight fraction w_w (3.00, 32.07, and 70.89% w/w). Similar study has also been done in the case of the NH_2^+ , CH_2 , and CF_3 chemical groups in $([\text{Pyrr}][\text{CF}_3\text{COO}] + \text{H}_2\text{O})$ binary system for the water weight fraction close to $w_w = 2.20\%$ w/w. Experimental data were then fitted according to eq 10 and are illustrated in Figure 12.

$$D(T) = D_0 \exp(E_a/RT) \quad (10)$$

where D_0 ($\text{m}^2\cdot\text{s}^{-1}$) is a pre-exponential factor and E_a ($\text{J}\cdot\text{mol}^{-1}$) is the activation energy for the diffusion process. Best-fit values are reported in Table 2.

For all the studied ionic species, each calculated activated energy E_a was found to be of the same order of magnitude, which is close to $14.0 \pm 0.8 \text{ kJ}\cdot\text{mol}^{-1}$ in the whole composition range in the case of the NH_2^+ and HSO_4^- groups. But, in the case of the $-\text{CH}_2$ group on the pyrrolidinium cation, the activated energy E_a increases with the water composition from 14.9 to $17.5 \text{ kJ}\cdot\text{mol}^{-1}$ for water weight fraction w_w ranging from 3.00 to 70.89% w/w, respectively. This behavior was expected since the diffusion is mainly controlled by the viscosity of the

Table 2. Arrhenius Equation Parameters (D_0 and E_a) for the Self-Diffusion Coefficients of the Different Ions or Chemical Groups in ([Pyrr][HSO₄] + H₂O) and ([Pyrr][CF₃COO] + H₂O) Binary Systems^a

w_w (% w/w)	chemical group	D_0 (m ² ·s ⁻¹)	E_a (kJ·mol ⁻¹)	R^2
([Pyrr][HSO ₄] + H ₂ O) Binary System				
3.00	NH ₂ ⁺ from [Pyrr]	6.15×10^{-9}	13.25	0.99321
	CH ₂ from [Pyrr]	3.22×10^{-9}	14.90	0.99428
	OH from [HSO ₄]	2.72×10^{-9}	14.27	0.99266
32.07	NH ₂ ⁺ from [Pyrr]	8.98×10^{-8}	14.31	0.92832
	CH ₂ from [Pyrr]	1.23×10^{-7}	16.22	0.87419
	OH from [HSO ₄]	1.11×10^{-7}	13.39	0.96299
70.89	NH ₂ ⁺ from [Pyrr]	3.62×10^{-7}	13.97	0.98834
	CH ₂ from [Pyrr]	9.38×10^{-7}	17.46	0.96542
	OH from HSO ₄	5.62×10^{-7}	14.73	0.98682
([Pyrr][CF ₃ COO] + H ₂ O) Binary System				
2.20	NH ₂ ⁺ from Pyrr	11.20×10^{-9}	12.10	0.98254
$T < 55\text{ }^\circ\text{C}$	CH ₂ from [Pyrr]	11.23×10^{-9}	12.80	0.98839
	CF ₃ from [CF ₃ COO]	25.68×10^{-9}	15.00	0.97360
$T > 55\text{ }^\circ\text{C}$	NH ₂ ⁺ from [Pyrr]	3.09×10^{-4}	39.80	0.99756
	CH ₂ from [Pyrr]	8.39×10^{-4}	43.00	0.99658
	CF ₃ from [CF ₃ COO]	3.20×10^{-4}	40.10	0.99870

^a R^2 is the correlation coefficient resulting from the fit procedure.

media, as shown and commented here in the conductivity and viscosity parts.

The separation of the temperature dependence D into the kinetic potential (hard sphere) and the (attractive) potential contributions can be achieved according to the activation energies. The activation energy for the self-diffusion at constant density can be decomposed into

$$E_D = -R \left(\frac{\partial \ln D}{\partial (1/T)} \right) = E_{\text{pot}} + E_{\text{kin}} \quad (11)$$

where E_{pot} is the potential contribution and the E_{kin} the kinetic contribution introduced as

$$E_{\text{kin}} = -R \left(\frac{\partial \ln D_{\text{HS}}}{\partial (1/T)} \right) = \frac{1}{2} RT \quad (12)$$

where R is the gas constant and D_{HS} is the self-diffusion coefficient for a dilute hard-sphere, $1/2RT = 2.47\text{ kJ}\cdot\text{mol}^{-1}$.

From this, in the liquid state, the E_{pot} value for ([Pyrr][HSO₄] + H₂O) binary system has been determined to be $14\text{--}17\text{ kJ}\cdot\text{mol}^{-1}$, reflecting the temperature effect on the acidic equilibrium of HSO₄⁻ anion at high water concentration.⁵⁸ In the case of the ([Pyrr][CF₃COO] + H₂O) binary system for $T > 55\text{ }^\circ\text{C}$, the E_{pot} value was found to be higher and close to $42.5 \pm 0.5\text{ kJ}\cdot\text{mol}^{-1}$, which reflects the strong interaction between the trifluoroacetate anion with the pyrrolidinium cation. This confirms also our observations in the previous paragraph.

4. CONCLUSION

In this work, transport mobilities of ions have been investigated in each case through the Stokes–Einstein equation. From this, the proton conduction in these PILs follows a combination of Grotthuss and vehicle-type mechanisms, which depends also on the water composition in solution. Self-diffusion coefficients (D) of the ion species in two (PILs + water) binary systems

with pyrrolidinium hydrogen sulfate and pyrrolidinium trifluoroacetate as PILs were determined by observing ¹H and ¹⁹F nuclei with the pulsed-field gradient spin-echo NMR technique. Results show that the diffusion of each proton depends on the system composition. The comparison between ions' mobility determined by conductivity and by NMR measurements indicates that the conductivity mechanism (Grotthuss or vehicle) depends also on the composition. This result was then correlated to the deviation from the ideality of viscosities for (PILs + water) systems as a function of the water weight fraction. [Pyrr][HSO₄] and [Pyrr][CF₃COO] PILs present opposed comportment in water. In the case of the [Pyrr][CF₃COO], viscosities, conductivities, self-diffusion coefficients (D), and the (attractive) potential E_{pot} indicate that the diffusion of each ion is similar. In other words, these ions are tightly bound together as ion pairs, reflecting in fact the importance of the hydrogen bonds in this PIL, whereas in the case of the [Pyrr][HSO₄], the strong H-bond between the HSO₄⁻ anion and water promotes a drastic change on the viscosity of the aqueous solution as well as on the conductivity which is up to $187\text{ mS}\cdot\text{cm}^{-1}$ for water weight fraction close to 60% at 298 K.

AUTHOR INFORMATION

Notes

The authors declare no competing financial interest.

ACKNOWLEDGMENTS

This research was supported by “Conseil Régional de la région Centre” through the SupCaplip project.

REFERENCES

- (1) Sadeghi, R.; Shekaari, H.; Hosseini, R. *J. Chem. Thermodyn.* **2009**, *41*, 273.
- (2) Garcia-Miaja, G.; Troncoso, J.; Romani, L. *J. Chem. Thermodyn.* **2009**, *41*, 161.
- (3) Letcher, T. M.; Reddy, P. *J. Chem. Thermodyn.* **2009**, *37*, 415.
- (4) Pal, A.; Gaba, R.; Singh, T.; Kumar, A. *J. Mol. Liq.* **2010**, *154*, 41.
- (5) Garcia-Miaja, G.; Troncoso, J.; Romani, L. *J. Chem. Thermodyn.* **2009**, *41*, 334.
- (6) Rilo, E.; Pico, J.; Garcia-Garabal, S.; Varela, L. M.; Cabeza, O. *Fluid Phase Equilib.* **2009**, *285*, 83.
- (7) Garcia-Miaja, G.; Troncoso, J.; Romani, L. *Fluid Phase Equilib.* **2008**, *274*, 59.
- (8) Rodriguez, H.; Brennecke, J. F. *J. Chem. Eng. Data* **2006**, *51*, 2145.
- (9) Li, J. G.; Hu, Y. F.; Sun, S. F.; Liu, Y. S.; Liu, Z. C. *J. Chem. Thermodyn.* **2010**, *42*, 904.
- (10) Earle, J. M.; Seddon, K. R. *Pure Appl. Chem.* **2000**, *72*, 1391.
- (11) Muginova, S. V.; Galimova, A. Z.; Polyakov, A. E.; Shekhovtsova, T. N. *J. Chem. Thermodyn.* **2010**, *65*, 331.
- (12) Greaves, T. L.; Drummond, C. J. *Chem. Rev.* **2008**, *108*, 206.
- (13) Gilli, P.; Pretto, L.; Bertolasi, V.; Gilli, G. *Acc. Chem. Res.* **2008**, *42*, 33.
- (14) Zarei, H. A.; Jalili, F. *J. Chem. Thermodyn.* **2007**, *39*, 55.
- (15) Rilo, E.; Ferreira, A. G. M.; Fonseca, I. M. A.; Cabeza, O. *Fluid Phase Equilib.* **2010**, *296*, 53.
- (16) Zhao, Y.; Zhang, X.; Zeng, S.; Zhou, Q.; Dong, H.; Tian, X.; Zhang, S. *J. Chem. Eng. Data* **2010**, *55*, 3513.
- (17) Lei, Z.; Yuan, J.; Zhu, J. *J. Chem. Eng. Data* **2010**, *55*, 4190.
- (18) Ahmady, A.; Hashim, M. A.; Aroua, M. K. *J. Chem. Eng. Data* **2010**, *55*, 5733.
- (19) Geng, Y.; Chen, S.; Wang, T.; Yu, D.; Peng, C.; Liu, H.; Hu, Y. *J. Mol. Liq.* **2008**, *143*, 100.

- (20) Andreatta, A.; Arce, A.; Rodil, E.; Soto, A. *J. Solution Chem.* **2010**, *39*, 371.
- (21) Arce, A.; Rodil, E.; Soto, A. *J. Solution Chem.* **2006**, *35*, 63.
- (22) Bhujrajh, P.; Deenadayalu, N. *J. Solution Chem.* **2007**, *36*, 631.
- (23) Calvar, N.; González, B.; Domínguez, A.; Tojo, J. *J. Solution Chem.* **2006**, *35*, 1217.
- (24) Domańska, U.; Laskowska, M. *J. Solution Chem.* **2008**, *37*, 1271.
- (25) Domańska, U.; Laskowska, M. *J. Solution Chem.* **2009**, *38*, 779.
- (26) Domańska, U.; Pobudkowska, A.; Wiśniewska, A. *J. Solution Chem.* **2006**, *35*, 311.
- (27) Gaillon, L.; Sirieix-Plenet, J.; Letellier, P. *J. Solution Chem.* **2004**, *33*, 1333.
- (28) Heintz, A.; Klasen, D.; Lehmann, J.; Wertz, C. *J. Solution Chem.* **2005**, *34*, 1135.
- (29) Iglesias-Otero, M.; Troncoso, J.; Carballo, E.; Román, L. *J. Solution Chem.* **2007**, *36*, 1219.
- (30) Liu, W.; Zhao, T.; Zhang, Y.; Wang, H.; Yu, M. *J. Solution Chem.* **2006**, *35*, 1337.
- (31) Marczak, W.; Verevkin, S. P.; Heintz, A. *J. Solution Chem.* **2003**, *32*, 519.
- (32) Anouti, M.; Caillon-Caravanier, M.; Dridi, Y.; Jacquemin, J.; Hardacre, C.; Lemordant, D. *J. Chem. Thermodyn.* **2009**, *41*, 799.
- (33) Anouti, M.; Vigeant, A.; Jacquemin, J.; Brigouleix, C.; Lemordant, D. *J. Chem. Thermodyn.* **2010**, *42*, 834.
- (34) Iglesias, M.; Torres, A.; Gonzalez-Olmos, R.; Salvatierra, D. *J. Chem. Thermodyn.* **2008**, *40*, 119.
- (35) Aihara, Y.; Bando, T.; Nakagawa, H.; Yoshida, H.; Hayamizu, K.; Akiba, E.; Price, W. S. *J. Electrochem. Soc.* **2004**, *151*, A119.
- (36) Aihara, Y.; Sugimoto, K.; Price, W. S.; Hayamizu, K. *J. Chem. Phys.* **2000**, *113*, 1981.
- (37) Hayamizu, K.; Aihara, Y.; Arai, S.; Martinez, C. G. *J. Phys. Chem. B* **1999**, *103*, 519.
- (38) Anouti, M.; Caillon-Caravanier, M.; Dridi, Y.; Galiano, H.; Lemordant, D. *J. Phys. Chem. B* **2008**, *112*, 13335.
- (39) Stejskal, E. O.; Tanner, J. E. *J. Chem. Phys.* **1965**, *42*, 288.
- (40) Ananikov, V. P. *Chem. Rev.* **2011**, *111*, 418.
- (41) Tanner, J. E. *J. Chem. Phys.* **1970**, *52*, 2523.
- (42) Cotts, R. M.; Hoch, M. J. R.; Sun, T.; Markert, J. T. *J. Magn. Reson.* **1989**, *83*, 252.
- (43) Molenat, J. *J. Chim. Phys. Physico-Chim. Biol.* **1969**, *66*, 825.
- (44) Claes, P.; Loix, Y.; Glibert, J. *Electrochim. Acta* **1983**, *28*, 421.
- (45) Vila, J.; Rilo, E.; Segade, L.; Cabeza, O.; Varela, L. M. *Phys. Rev. E* **2005**, *71*, 031201.
- (46) Bockris, J. O'M.; Reddy, A. K. N. *Modern Electrochemistry*; Plenum Press: New York, 1998; Vol. 1, Chapter 4.
- (47) Anouti, M.; Jones, J.; Boisset, A.; Jacquemin, J.; Caillon-Caravanier, M.; Lemordant, D. *J. Colloid Interface Sci.* **2009**, *340*, 104.
- (48) Robinson, R. A.; Stokes, R. H. *Electrolyte Solutions*; Butterworths: London, 1965.
- (49) Hiemenz, P. C.; Rajagopalan, R. *Principles of Colloid and Surface Chemistry*; Marcel Dekker Inc.: New York, 1997.
- (50) Anouti, M.; Jacquemin, J.; Lemordant, D. *Fluid Phase Equilib.* **2010**, *297*, 13.
- (51) Seddon, K. R.; Stark, A.; Torres, M. J. *Pure Appl. Chem.* **2000**, *72*, 2275.
- (52) Singh, T.; Kumar, A. *J. Phys. Chem. B* **2007**, *111*, 7843.
- (53) Rollet, A.-L.; Porion, P.; Vaultier, M.; Billard, I.; Deschamps, M.; Bessada, C.; Jouvencal, L. *J. Phys. Chem. B* **2007**, *111*, 11888.
- (54) Umecky, T.; Kanakudo, M.; Ikushima, Y. *Fluid Phase Equilib.* **2005**, *329*, 288.
- (55) Fraser, K. J.; Izgorodina, E. I.; Forsyth, M.; Scott, J. L.; MacFarlane, D. R. *Chem. Commun.* **2007**, *37*, 3817.
- (56) Noda, A.; Hayamizu, K.; Watanabe, M. *J. Phys. Chem. B* **2001**, *105*, 4603.
- (57) Driver, G.; Johnson, K. E. *Green Chem.* **2003**, *5*, 163.
- (58) Yoshida, K.; Matubayasi, N.; Nakahara, M. *J. Chem. Phys.* **2007**, *126*, 089901.